European Radiology (2019) 29:362–372
https://doi.org/10.1007/s00330-018-5574-0

HEPATOBILIARY-PANCREAS

CT prediction of resectability and prognosis in patients with pancreatic ductal adenocarcinoma after neoadjuvant treatment using image findings and texture analysis

Bo Ram Kim[1] · Jung Hoon Kim[1,2] · Su Joa Ahn[1] · Ijin Joo[1] · Seo-Youn Choi[3] · Sang Joon Park[1] · Joon Koo Han[1,2]

Received: 30 March 2018 / Revised: 21 May 2018 / Accepted: 29 May 2018 / Published online: 21 June 2018

Abstract

Objectives To assess utility of CT findings and texture analysis for predicting the resectability and prognosis in patients after neoadjuvant therapy for pancreatic ductal adenocarcinoma (PDAC).

Materials and methods Among 308 patients, 45 with PDAC underwent neoadjuvant therapy (concurrent-chemoradiation-therapy, CCRT, n = 27 and chemotherapy, ChoT, n = 18) before surgery were included. All underwent baseline and preoperative CT. Two reviewers assessed CT findings and resectability. We analyzed relationship between CT resectability and residual tumor. CT texture values obtained by subtracting preoperative from baseline CT were analyzed using multivariate Cox/logistic regression analysis to identify significant parameters predicting resectability and prognosis.

Results There were 30 patients without residual tumor (CCRT, n = 20; ChoT, n = 10) and 15 with residual tumor (CCRT, n = 7; ChoT, n = 8). Considering borderline as resectable was more accurate for R0 resectability than considering borderline as unresectable (68.9% vs 55.6% and 51.1%, $p < 0.001$). Particularly, neoadjuvant CCRT provided better accuracy than that in ($p < 0.001$). In CT texture analysis, higher subtracted entropy (cut-off: 0.03, HR 0.159, $p = 0.005$) and lower subtracted GLCM entropy (cut-off: –0.35, HR 10.235, $p = 0.036$) are important parameters for prediction of longer overall survival.

Conclusion CT findings with texture analysis can be useful for predicting a patient's outcome, including resectability and prognosis, after neoadjuvant therapy for PDAC.

Key Points

- *Considering borderline resectable tumor as resectable have better accuracy for resectability.*
- *Considering borderline as resectable, CCRT-patients have better resectability accuracy than chemotherapy-patients.*
- *Higher subtracted entropy and lower subtracted GLCM entropy are predictors of favorable outcome.*

Keywords Pancreatic neoplasm · Neoadjuvant therapy · Pancreatectomy · Prognosis · Diagnosis

✉ Jung Hoon Kim
jhkim2008@gmail.com

[1] Department of Radiology, Seoul National University Hospital, 101 Daehangno, Jongno-gu, Seoul 110-744, Republic of Korea

[2] Institute of Radiation Medicine, Seoul National University College of Medicine, Seoul, Korea

[3] Department of Radiology, Soonchunhyang University Bucheon Hospital, Bucheon, Korea

Abbreviations

ASM	Angular second moment
CA	Celiac axis
CCRT	Concurrent chemoradiation therapy
GLCM	Grey level co-occurrence matrices
HR	Hazard ratio
IDM	Inverse difference moment
OS	Overall survival
PV	Portal vein
SMV	Superior mesenteric vein

Introduction

Despite all the efforts to develop a better treatment strategy for pancreatic ductal adenocarcinoma (PDAC), the prognosis still remains poor. The 5-year survival rate is 8% for pancreas cancer, even after successful surgical resection, and the 5-year patient survival rate does not exceed 20% [1, 2]. Moreover, 30% of resected PDACs have a positive resection margin [2]. The resection margin status is essential for determining a patient's prognosis. Patients who undergo R1 resection, which is gross total resection with a histologically positive margin, or R2 resection, which is resection with residual gross tumor, have a worse chance of survival than that those who undergo R0 resection, which is gross total resection with a histologically negative margin, and with a better survival outcome [3–5].

After the emerging concept of borderline resectable PDAC, several studies have reported that neoadjuvant treatment could downstage the tumor and, therefore, offer the opportunity for surgery with R0 resection [6–8]. In this respect, accurate imaging-based assessment of the resectability before and after neoadjuvant treatment is crucial for therapeutic management. CT is the image of choice for preoperative staging and resectability assessment in PDAC with 95% [9] or 81% positive predictive value [10]. However, achieving a sufficient accuracy for precise assessment has been challenging. Furthermore, neoadjuvant treatment significantly reduces the diagnostic performance of CT for the prediction of resectability because of changes after neoadjuvant treatment, including pancreatitis, necrosis or fibrous scar [11–14].

Recently, CT texture analysis has warranted much attention as quantitative imaging biomarkers in oncologic imaging, providing important information regarding tumor characterization and prognosis by quantifying tissue heterogeneity, and assessing the distribution of texture coarseness [15–17]. According to previous studies, texture analysis is helpful for predicting the prognosis or assessing the therapeutic response in various cancers [16, 18, 19].

To our knowledge, there have been no published reports regarding the usefulness of CT texture analysis for predicting resectability and the prognosis after neoadjuvant treatment in patients with PDAC. The purpose of our study is to assess the utility of CT findings and texture analysis for predicting resectability after neoadjuvant therapy in patients with PDAC. We also assessed the utility of CT texture analysis for predicting the patient prognosis after surgery.

Materials and methods

This retrospective study was approved by our institutional review board and the requirement for patient informed consent was waived.

Study population

From January 2013 to February 2016, a total of 308 patients with pathologically proven PDAC underwent surgery. Among them, 48 patients received neoadjuvant treatment because the tumor was considered as borderline resectable or locally advanced on the baseline CT images. Exclusion criteria were as follows: (a) patients who did not have preoperative CT after neoadjuvant treatment (n = 1); (b) reconstruction technique mismatch between the baseline and preoperative CT (n = 2). Therefore, a total of 45 patients (23 men, 22 women; mean age, 64.8 ±8.7 years) who underwent concurrent chemoradiation therapy (CCRT, n = 27) or neoadjuvant chemotherapy (n = 18) were included in our study population (Fig. 1). All patients included in our study underwent baseline CT and preoperative CT; the mean interval between the baseline CT and the preoperative CT scan was 160.7 days. The mean interval between preoperative CT scan and surgical resection was 16.2 days.

Chemotherapy was performed using the following regimens: oxaliplatin, irinotecan, fluorouracil and leucovorin (FOLFIRINOX) in seven patients; gemcitabine-based chemotherapy in 11 patients (gemcitabine alone [n = 3], gemcitabine and cisplatin [n = 3], gemcitabine and xeloda [n = 2], gemcitabine and oxaliplatin [n = 1], gemcitabine and tarceva [n = 2]). Neoadjuvant CCRT consisted of 45Gy/25fx + 9Gy/5fx (n = 18) or 45Gy/25fx + 5.4Gy/5fx (n = 9) of external-beam radiation and weekly gemcitabine- (n = 22), fluorouracil- (n = 3) or capecitabine-based (n = 2) chemotherapy. Surgery was performed using pylorus-preserving pancreaticoduodenectomy (n = 25), Whipple operation (n = 8), distal pancreatectomy (n = 11), total pancreatectomy (n = 4), palliative surgery (n = 3) or opening and closure (n = 5). Twenty-nine patients received postoperative chemotherapy, 10 patients received chemoradiation therapy and 4 patients did not receive postoperative treatment. The remaining two patients were followed up at outside hospitals and had no record of the postoperative treatment.

MDCT examination

The CT examination was performed using either quadruple-phase CT (n = 45) which consisted of unenhanced, early arterial, pancreatic and venous phases or using triple-phase CT (n = 9) which consisted of unenhanced, arterial and venous phases. Baseline and preoperative CT scans were obtained using one of the following commercially available MDCT scanners: 16-MDCT scanner (Sensation 16; Siemens Healthineers [n = 8]), 64-MDCT scanner (Brilliance 64; Philips [n = 8]; SOMATOM Definition; Siemens Healthineers [n = 5]; Discovery CT750 HD; GE Healthcare [n = 3]), 128-MDCT scanner (Ingenuity, Philips Healthcare [n = 5]) or a 320-MDCT scanner (Aquilion ONE; Canon

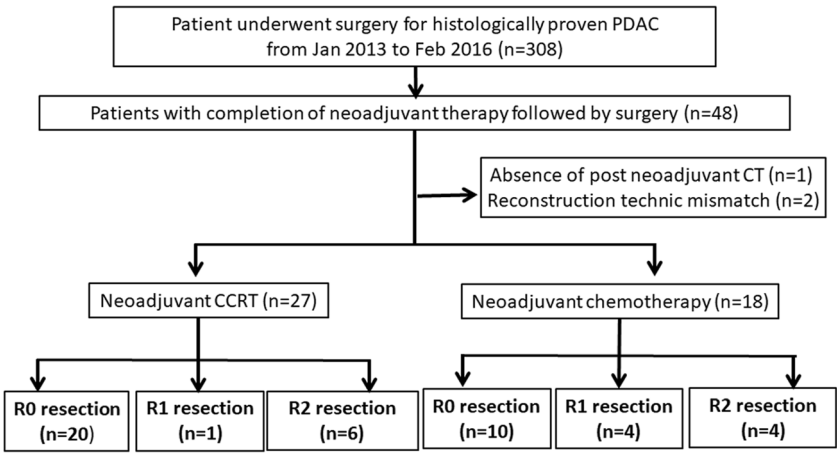

Fig. 1 Flow chart schematizing the patient selection process. PDAC = pancreatic ductal adenocarcinoma, CT = computed tomography, CCRT = concurrent chemoradiation therapy

Medical Systems [n = 16]). CT scanners used in baseline and preoperative CT were matched in 13 of 45 patients.

Detailed information regarding the CT parameters are summarized in Table 1. A total of 1.5 mL of non-ionic contrast material, i.e. iopromide solution containing 370 mg of iodine per millilitre per kilogram of body weight was administered using a power injector (Stellant CT; Medrad) at a rate of 3 mL/sec with an 18-gauge intravenous catheter into the antecubital vein, followed by a 20-mL saline flush. For image acquisition, an automatic bolus tracking technique was used. The trigger threshold was 100 HU at the abdominal aorta. Early arterial phase images were obtained 6 seconds after the trigger threshold was achieved and pancreatic phase images were obtained 5–9 seconds later. The average imaging time delay was 23 seconds for the early arterial phase, 37–45 seconds for the pancreatic phase and 70 seconds for the venous phase.

CT image analysis

For each patient, baseline and preoperative CT images were reviewed by two radiologists (I.J and S.J.A with ten and eight years of clinical experience with abdominal imaging, respectively). Both reviewers were blinded to the history as well as the operative and histological findings, although they were aware that the patients had PDAC. They assessed the imaging findings and classified tumors as resectable, borderline resectable or unresectable. We categorized the tumor–vessel interface as four grades, i.e. absence, abutment (≤180 degrees of the circumference), encasement (>180 degrees of the circumference and luminal irregularity), and occlusion. A tumor with one or more of the following criteria was classified as borderline resectable tumor: (a) short segment narrowing or occlusion of the superior mesenteric vein (SMV) or portal vein (PV) that is amenable to resection and venous reconstruction; (b) abutment or short segmental encasement of the hepatic artery or branches; (c) abutment of the SMA; (d) abutment of celiac axis (CA) [20–22].

The reference standard for determining the accuracy of the resectability was the histopathologic and surgical findings. We used the R classification for residual tumors, according to the International Union Against Cancer: no residual tumor (R0); microscopic residual tumor (R1) or macroscopic residual tumor (R2) [23]. Lesions that were interpreted as resectable tumors were regarded as pathologic R0 resection and lesions

Table 1 Scanning parameters of contrast-enhanced multi-detector row computed tomography

Parameter	Sensation 16	Brilliance 64	Definition	Discovery	Ingenuity	Aquilion ONE
No. of channels	16	64	64	64	128	320
Section collimation*	16 × 0.75	64 × 0.625	64 × 0.625	64 × 0.625	64 × 0.625	64 × 0.5
Section thickness	3	2.5–3.2	2.5–3.2	2.5–3.2	3	2.5–3.2
Reconstruction interval	3	3	3	3	3	3
Pitch	1.25	0.9–1.2	0.9–1.2	0.9–1.2	1.172	0.813
Rotation time (sec)	0.5	0.75	0.5	0.5	0.5	0.5
Tube voltage (kVp)	120	120	120	120	120	120
Field of view	300–370	300–370	300–370	300–370	300–370	300–370

Tube current was adjusted using automatic tube current modulation

*Number of detector rows times section thickness (mm)

interpreted as unresectable tumors were regarded as pathologic R1 or R2 resection. Borderline tumors in CT-based interpretation were statistically categorized on both sides for two consecutive resectability analysis: (a) Borderline resectable tumors were classified as resectable tumors, considering R0 resection was feasible; (b) On the contrary, borderline unresectable tumors were classified as unresectable tumors.

Computerized CT texture analysis

CT texture analysis was performed using computer-based, in-house software (MISSTA, Medical Imaging Solution for Segmentation and Texture Analysis) with fully automated quantification of the texture features implemented using dedicated C++ language (Microsoft Foundation Classes; Microsoft). Because significant results of texture analysis of PDAC were predominantly shown at venous phase in previous studies [17, 24] , venous-phase images were selected for this study to maintain the consistency of the texture analysis results. In order to overcome the limitation of defining the boundary of PDAC, a radiologist (J.H.K) who was not involved in the texture analysis drew a region of interest (ROI) along the margin of the tumor on the baseline and preoperative CT, respectively, at the same level as possible, prior to segmentation for the texture analysis. The ROI was drawn in the CT image where the tumor was most clearly depicted, regardless of phase. In all cases, enhancement difference existed between surrounding pancreatic parenchyma and tumor. In cases with unclear tumor-parenchyma enhancement difference, ancillary features such as pancreatic duct or bile duct cut-off were additionally used for drawing the ROI. Subsequently, another radiologist (B.R.K) performed three repetitive segmentations of the tumor, based on the ROI drawn of pancreatic phase or venous phase, using the texture analysis software program (Fig. 2). In order to minimize measurement errors, we used the mean value of texture parameters obtained from three respective segmentations of the same representative lesion. After the lesion was segmented, the program automatically calculated the following texture parameters: histogram parameters including: (a) mean attenuation; (b) standard deviation and variance of the grey-level (degree of variation from the mean pixel value); (c) skewness (asymmetry); (d) kurtosis (bulging or peakedness); (e) entropy (irregularity); (f) homogeneity (distribution of grey level); (g) surface area; (h) sphericity; and (i) discrete compactness (ratio of the contact surface area-to-the maximum contact surface area); as well as the second-order texture parameters based on grey-level co-occurrence matrices (GLCM) including: (a) GLCM moments, (b) the GLCM angular second moment (ASM; textural uniformity), (c) GLCM inverse difference moment (IDM; influenced by the homogeneity), (d) GLCM contrast (contrast or local intensity variation) and (e) GLCM entropy (randomness, disorder), and which characterize the spatial distribution of grey levels in images [25].

Statistical analysis

Categorical data were expressed as numbers and compared using the Chi-squared test or Fisher's exact test. Quantitative data were expressed as the mean ± standard deviation and were compared using independent sample *t* tests. Logistic regression analysis was used to identify significant predictors of R0 resection. The paired *t* test and the Wilcoxon signed rank test were performed for comparison of the baseline CT texture parameters and the preoperative CT texture parameters after the Shapiro–Wilk test. Subtracted texture values determined by subtracting the baseline CT from the preoperative CT texture parameters were calculated. The Cox proportional hazards regression model was utilized to evaluate the effect of subtracting texture parameters and clinico-pathologic variables on patient overall survival (OS). In order to assess inter-observer agreement, we performed a simple κ analysis. The degree of interobserver agreement in the range of 0.81–1.00 was interpreted as excellent, 0.61–0.80 as substantial, 0.41–0.60 as moderate, 0.21–0.40 as fair and 0.00–0.20 as poor. The SPSS 21.0 software package (SPSS, IBM) was used for all statistical analyses in our study, and a p value of <0.05 was considered to be a statistically significant difference.

Results

The patient characteristics are shown in Table 2. Twenty patients were classified as R0, one as R1 and six as R2 in the neoadjuvant CCRT group, and 10 patients were classified as R0, four as R1 and four as R2 in the neoadjuvant chemotherapy group. The mean CA of 19-9 decreased after neoadjuvant treatment from 1317.4 ±2394.2 U/mL to 572.3 ±1955.0 U/mL, and the tumor size also decreased from 30.9 ±9.7 mm to 22.2 ±8.7 mm. During the follow-up period, tumor recurred in 33 patients (73.3%) and 12 patients (26.7%) had early recurrence within 1 year.

Accuracy of CT findings for predicting resectability after neoadjuvant therapy

Table 3 summarizes the diagnostic performance of CT for predicting the resectability after neoadjuvant therapy. Overall accuracy for R0 resectability was better when considering borderline as resectable tumor (68.9%) than when considering borderline as unresectable tumor (55.6% and 51.1%, $p < 0.001$). In particular, the CCRT group exhibited superior accuracy (77.8% vs. 51.9% for reader 1; 74.1% vs. 44.4% for reader 2, $p < 0.001$) regarding the resectability assessment when considering the borderline as resectable (Fig. 3). Inter-

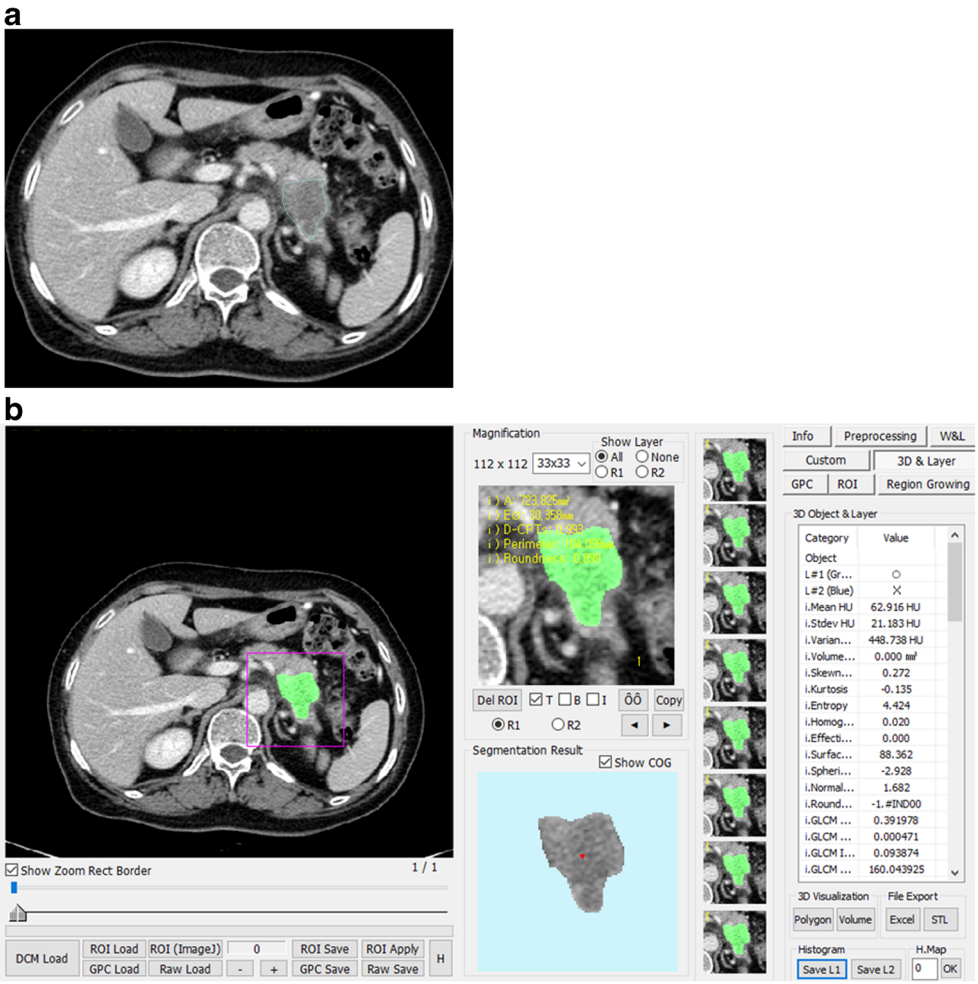

Fig. 2 CT texture analysis. **a** The outlining of pancreatic adenocarcinoma was manually conducted, prior to texture analysis. **b** Subsequently, segmentation was performed in a consensus manner by using an in-house texture analysis software program, and texture features of the nodules were automatically extracted and calculated

reader agreement of the tumor-vessels relationship evaluation between the two radiologists was moderate to substantial (0.559–0.664).

Accuracy of CT texture analysis for predicting resectability after neoadjuvant therapy

Table 4 shows the comparison of the texture parameters between baseline and after neoadjuvant therapy in the R0 resection group and the R1 or R2 resection group. In the R0 resection group, several parameters, including the surface area, sphericity, discrete compactness, GLCM ASM and GLCM entropy, showed a significant difference between the baseline and after neoadjuvant treatment ($p < 0.05$). In the R1 or R2 resection group, the same parameters, i.e. surface area, sphericity, discrete compactness, GLCM ASM and GLCM entropy, showed a significant difference between the baseline and after neoadjuvant treatment ($p < 0.05$). Regarding the subtracted texture values, the subtracted surface area was larger in the R0 resection group (–19.6 vs. –12.4 mm^2, $p = 0.273$) and subtracted GLCM contrast was higher in the residual tumor group (24.9 vs –86.5, $p = 0.09$). In multivariate logistic regression analysis, none of the preoperative CT texture parameters had significant association with resectability. However, using the subtracted texture values, the following features attained statistical significance for predicting the R0 resection: lower subtracted value of surface area (hazard ratio [HR] 1.077, $p = 0.011$), higher subtracted values of GLCM IDM (HR 0.000, $p = 0.005$) and GLCM contrast (HR 0.982, $p = 0.012$).

Important CT texture analysis for predicting overall survival after surgery

The median patient survival time was 23.9 ±2.1 months. The median survival time of the neoadjuvant chemotherapy group (24.7 ±6.3 months) was longer than that of the CCRT group (22.9 ±2.1 months) without a significant difference ($p = 0.772$). The entropy decreased after neoadjuvant treatment from 4.37 ± 0.22 to 4.27 ±0.22 ($p = 0.026$) and the GLCM entropy also decreased from 3.24 ±0.18 to 3.05 ±0.22 ($p = 0.000$). On multivariate analysis, the higher subtracted value of entropy (HR 0.159, $p = 0.005$) and lower subtracted value

Table 2 Characteristics of the study population

Characteristics	Values (n = 45)	R0 resection (n = 30)	R1 or R2 resection (n = 15)	*p* value*	Overall survival	
					Hazard ratio	*p* value†
Age (y)	64.8 ±8.7	62.5 ±8.3	69.5 ±7.8	**0.009**	1.016 (0.977, 1.056)	0.435
No. of men	23 (51.1%)	15 (50.0%)	8 (53.3%)	0.916	0.787 (0.390, 1.590)	0.505
CA 19-9 (U/mL)						
Baseline	1317.4 ±2394.2	1585.1 ±2862.0	781.9 ±766.6	0.294	1.000 (1.000, 1.000)	0.512
Post-neoadjuvant	572.3 ±1955.0	595.7 ±2253.9	525.4 ±1218.9	0.911	1.000 (1.000, 1.000)	0.695
Tumor location				0.490		
Head/neck	32 (71.1%)	23 (76.7%)	9 (60.0%)		3.273 (0.966, 11.083)	0.057
Body	6 (13.3%)	3 (10.0%)	3 (20.0%)		3.475 (0.797, 15.158)	0.097
Tail	7 (15.6%)	4 (13.3%)	3 (20.0%)		Reference category	
Tumor largest diameter (mm)						
Baseline	30.9 ±9.7	31.7 ±9.7	29.4 ±9.8	0.459	0.775 (0.511, 1.177)	0.232
Post-neoadjuvant	22.2 ±8.7	22.4 ±8.7	21.7 ±9.1	0.803	0.948 (0.630, 1.426)	0.798
T stage				**<0.001**		
T1	4 (8.9%)	4 (13.3%)	0 (0.0%)		Reference category	
T2	1 (2.2%)	1 (3.3%)	0 (0.0%)		0	0.987
T3	29 (64.4%)	23 (76.7%)	6 (40.0%)		3.781 (0.507, 28.223)	0.195
T4	3 (6.7%)	2 (6.7%)	1 (6.7%)		24.054 (2.310,250.488)	**0.008**
Palliative Op./O&C‡	8 (17.8%)	0 (0.0%)	8 (53.3%)		12.547 (1.545, 101.862)	**0.018**
Differentiation grade (n = 37)				0.477		
Well (G1)	6 (16.2%)	5 (16.2%)	1 (14.3%)		Reference category	
Moderately (G2)	26 (70.3%)	20 (66.7%)	6 (85.7%)		1.393 (0.405, 4.793)	0.6
Poorly (G3)	5 (13.5%)	5 (16.7%)	0 (0.0%)		3.046 (0.713, 13.013)	0.133
Presence of LVI (n = 37)	19 (51.4%)	15 (50.0%)	4 (57.1%)	0.936	1.492 (0.682, 3.264)	0.317
Presence of PNI (n = 37)	27 (73.0%)	23 (76.7%)	4 (57.1%)	0.565	5.199 (1.539, 17.566)	**0.008**
Presence of LN invasion (n = 37)	10 (16.2%)	7 (23.3%)	3 (42.9%)	0.565	1.245 (0.539,2.874)	0.608
Patient outcome (n = 45)						
Early recurrence	12 (26.7%)	5 (16.7%)	7 (46.7%)	**0.007**	7.914 (3.381,18.523)	**0**
Recurrence	33 (73.3%)	21 (70.0%)	12 (80.0%)	**0.005**	2.705 (1.044, 7.010)	**0.04**
Deaths	35 (77.8%)	21 (70.0%)	14 (93.3%)	0.163		

Statistically significant results are shown in bold in the table

**p* values were determined by independent *t* test or Pearson's chi-squared test or Fisher's exact test for comparison between the R0 group and R1 & R2 groups

† *p* values were determined by Cox proportional hazard model for overall survival

‡ O & C = open and closure operation

of GLCM entropy (HR 10.235, $p = 0.036$) were associated with a better outcome (Table 5, Fig. 4). The optimal cut-off values were 0.03 for the subtracted value of entropy and –0.35 for the subtracted value of GLCM entropy.

Table 3 Diagnostic performance of CT for prediction of resectability after neoadjuvant therapy in pancreatic cancer

	Neoadjuvant treatment	Accuracy (%)	Sensitivity (%)	Specificity (%)	PPV (%)	NPV (%)
Considering borderline resectable tumors as unresectable						
Reader 1	Chemotherapy	61.1 (11/18)	60.0 (6/10)	62.5 (5/8)	66.7 (6/9)	55.6 (5/9)
	CCRT	51.9 (14/27)	40.0 (8/20)	85.7 (6/7)	88.9 (8/9)	33.3 (6/18)
	Overall	**55.6 (25/45)**	46.7 (14/30)	73.3 (11/15)	77.8 (14/18)	40.7 (11/27)
Reader 2	Chemotherapy	61.1 (11/18)	40.0 (4/10)	87.5 (7/8)	80.0 (4/5)	53.8 (7/13)
	CCRT	44.4 (12/27)	30.0 (6/20)	85.7 (6/7)	85.7 (6/7)	30.0 (6/20)
	Overall	**51.1 (23/45)**	33.3 (10/30)	86.7 (13/15)	83.3 (10/12)	39.4 (13/33)
Considering borderline resectable tumors as resectable						
Reader 1	Chemotherapy	55.6 (10/18)	90.0 (9/10)	12.5 (1/8)	56.3 (9/16)	50.0 (1/2)
	CCRT	**77.8 (21/27)**	90.0 (18/20)	42.9 (3/7)	81.8 (18/7)	60.0 (3/5)
	Overall	**68.9 (31/45)**	90.0 (27/30)	26.7 (4/15)	71.1 (27/38)	57.1 (4/7)
Reader 2	Chemotherapy	61.1 (11/18)	80.0 (8/10)	37.5 (3/8)	61.5 (8/13)	53.8 (3/5)
	CCRT	**74.1 (20/27)**	80.0 (16/20)	57.1 (4/7)	84.2 (16/19)	50.0 (4/8)
	Overall	**68.9 (31/45)**	80.0 (24/30)	46.7 (7/15)	75.0 (10/12)	53.8 (7/13)

Neoadjuvant CCRT provided better accuracy than that in the chemotherapy group, when considering borderline resectable tumors as resectable. The result and the oversall accuracy was shown in bold

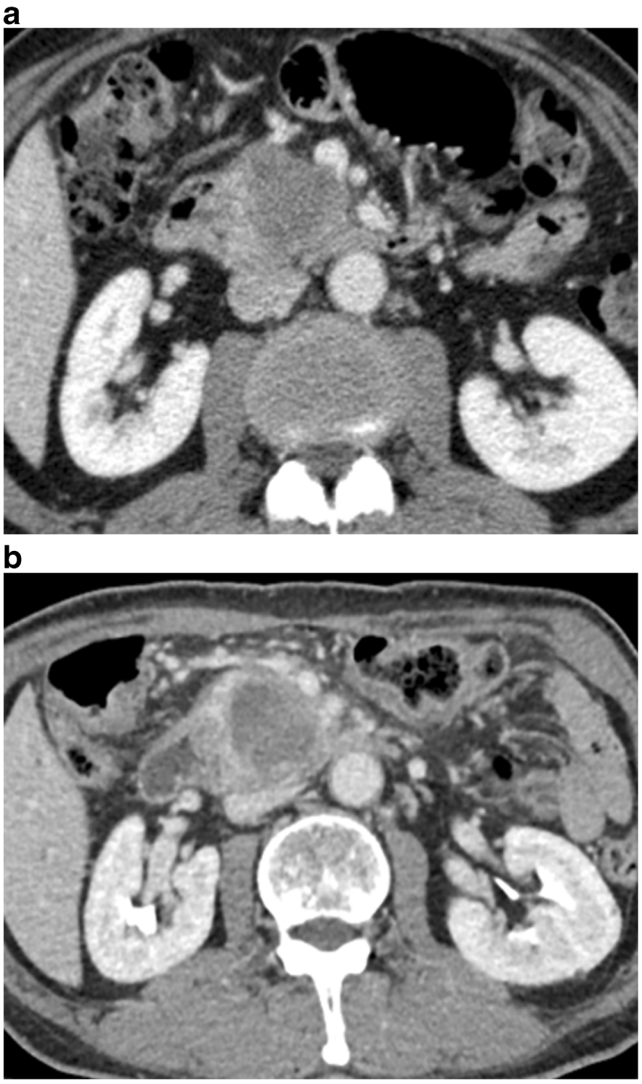

Fig. 3 **a** Baseline CT image of a 4-cm pancreatic ductal adenocarcinoma in a 62-year-old man before neoadjuvant CCRT shows pancreas head cancer abutment of SMV and SMA. **b** After completion of neoadjuvant CCRT, preoperative CT still shows abutment of SMV and SMA with increased peri-tumoural and perivascular infiltration. The tumor was classified as a borderline resectable tumor by both readers. However, postoperative histological examination revealed that R0 resection was performed without a microscopic residual tumor

Discussion

In our study, after neoadjuvant therapy, considering the borderline as resectable tumor has better accuracy for R0 resectability than considering the borderline as unresectable tumor (68.9% vs 55.6% and 51.1%). In particular, the neoadjuvant CCRT group provided better accuracy (77.8%, 74.1%) than the chemotherapy group (55.6%, 61.1%).

Previous studies [11–14, 26, 27] demonstrated the decreased diagnostic performance of CT for the evaluation of resectability after neoadjuvant treatment. Katz et al [26] suggested that radiographic downstaging was uncommon; only

Table 4 Comparison of CT texture parameters between baseline and after neoadjuvant therapy in R0 resection group and R1 or R2 resection group

	Total (n = 45)			R0 resection group (n = 30)			R1 or R2 resection group (n = 15)		
	Baseline	Preoperative	*p* value	Baseline	Preoperative	*p* value	Baseline	Preoperative	*p* value
Average mean HU	76.74 ±17.34	75.76 ±16.88	0.708	77.46 ±18.37	76.35 ±15.81	0.723	75.27 ±15.48	74.52 ±19.40	0.880
SD (HU)	21.88 ±5.21	21.97 ±5.15	0.919	21.11 ±4.24	22.11 ±5.18	0.418	23.43 ±6.62	21.69 ±5.28	0.240
Variance (HU)	505.30 ±255.08	509.84 ±253.85	0.925	462.87 ±191.90	516.37 ±248.96	0.360	590.19 ±341.50	496.79 ±271.78	0.281
Skewness	-0.02 ±0.31	0.15 ±0.84	0.376	-0.01 ±0.31	0.26 ±0.96	0.169	-0.02 ±0.31	-0.04 ±0.53	0.881
Kurtosis	0.29 ±0.56	1.06 ±5.76	0.87	0.30 ±0.60	1.37 ±7.06	0.398	0.25 ±0.47	0.34 ±0.75	0.706
Entropy	4.37 ±0.22	4.27 ±0.22	0.026	4.35 ±0.19	4.25 ±0.21	0.052	4.40 ±0.26	4.26 ±0.24	0.061
Homogeneity	0.02 ±0.01	0.02 ±0.01	0.524	0.02 ±0.08	0.02 ±0.01	0.476	0.02 ±0.01	0.02 ±0.01	0.538
Surface area	63.35 ±21.14	46.12 ±18.07	0.000	65.66 ±22.46	46.01 ±17.79	0.000	58.73 ±18.06	46.33 ±19.24	0.009
Sphericity	-2.57 ±0.65	-2.14 ±0.68	0.000	-2.57 ±0.67	-2.19 ±0.68	0.003	-2.56 ±0.68	-2.14 ±0.69	0.039
Discrete compactness	1.88 ±0.17	2.06 ±0.25	0.000	1.86 ±0.15	2.06 ±0.22	0.000	1.92 ±0.19	2.06 ±0.24	0.005
GLCM Moments	0.62 ±0.27	0.60 ±0.26	0.000	0.62 ±0.27	0.64 ±0.29	0.836	0.60 ±0.24	0.59 ±0.31	0.875
GLCM ASM	0.00 ±0.00	0.00 ±0.00	0.000	0.00 ±0.00	0.00 ±0.00	0.036	0.00 ±0.00	0.00 ±0.00	0.012
GLCM IDM	0.09 ±0.02	0.10 ±0.03	0.094	0.00 ±0.03	0.00 ±0.05	0.713	0.09 ±0.03	0.09 ±0.03	0.732
GLCM contrast	246.38 ±164.19	234.14 ±165.45	0.453	223.63 ±117.86	248.51 ±187.57	0.515	291.92 ±229.38	205.43 ±108.74	0.110
GLCM entropy	3.24 ±0.18	3.05 ±0.22	0.000	3.25 ±0.17	3.05 ±0.19	0.000	3.31 ±0.18	3.05 ±0.22	0.006

GLCM = grey-level co-occurrence matrices, ASM = angular second moment, IDM = inverse difference moment

Table 5 Multivariate Cox proportional hazards regression analysis for overall survival

Parameter	Hazard ratio	*p* value*
Entropy_subtraction	0.159 (0.044, 0.575)	0.005
GLCM Entropy_subtraction	10.235 (1.159, 90.409)	0.036

*p values were determined by the Cox proportional hazard model for overall survival

one of their patients (0.8%) was down-staged to resectable status among the 112 with borderline resectable PDAC after neoadjuvant treatment, and 95% R0 resection was achieved in 85 patients who underwent pancreatectomy with favourable median survival (33 vs. 22 months). Cassinotto et al [12, 14] determined that the CT accuracy of R0 resectability after neoadjuvant treatment was lower than that in the control group (58% vs 83%, $p = 0.039$) due to the overestimation of vascular invasion and they suggested that partial regression of tumor-SMV/PV contact was suitable for surgical treatment with a 100% positive predictive value for R0 resection. As in our study results, interpreting the borderline resectable tumor as a resectable tumor can provide superior accuracy of R0 resection after neoadjuvant treatment. Applying moderate criteria for vascular contact assessment could give superior accuracy of resectability assessment after neoadjuvant treatment. Therefore, it is useful to extend the range of the criteria for CT image-based resectability evaluation after neoadjuvant treatment.

Our CT texture analysis results revealed that subtracted values of the CT texture parameter can be useful to predict a patient's prognosis. These results suggested the implication of the texture parameter as the predictor of a patient's outcome, even though it is not a characteristic to improve resectability prediction. In our study, the higher subtracted value of entropy (optimal cut-off values were 0.03, HR 0.159, $p = 0.005$) and the lower subtracted value of GLCM entropy (optimal cut-off values were –0.35 HR 10.235, $p = 0.036$) are important parameters for predicting longer OS after surgery. The entropy is the first-order statistic from the grey-level histogram as it reflects how uniform the grey-level distribution is and what is texture irregularity. Higher entropy represents increased heterogeneity [28, 29]. According to previous studies, heterogeneous tumors which tended to have greater entropy showed tumor aggressiveness, poor treatment response or a poor patient prognosis [28, 30–32]. Focusing on changes before and after tumor treatment, Yip et al [33] suggested that the tumor texture of primary esophageal cancer became more homogeneous after neoadjuvant chemotherapy and with a significant decrease in entropy. Additionally, Goh et al. [19] reported that tumor entropy decreased by 3–45% after administration of the tyrosine kinase inhibitor in metastatic, renal cell carcinoma and baseline entropy (≤2.33) was correlated with the time to progression ($p = 0.02$). However, in our study results, a higher subtracted value of entropy was associated with a longer OS. Even though the mean tumor entropy was decreased after treatment from 4.37 to 4.27, our results regarding the relationship between survival times and the subtracted entropy differ from the results of previously published studies. This discrepancy might result from the different underlying tumor biology of different organs that determine the response to the neoadjuvant treatment. According to published histologic grading schemes of PDAC [34, 35], three variables are in consideration for evaluation of the treatment response of PDAC, i.e. viable tumor cell mass, fibrosis and necrosis. In the marked-response group, there were fewer remaining cancer cells, but more tumor was replaced by fibrosis or necrosis and more tumor cells had the cytopathic effect than in the poor response group. These kinds of heterogeneous changes may have contributed to the associated higher subtracted entropy value and the longer patient survival outcome. However, further studies regarding the relationship between texture parameters and histologic change in the post-neoadjuvant treatment clinical setting are warranted.

Whereas GLCM is second-order statistics that are grey-level, co-occurrence matrix calculated the spatial distribution of grey levels. The GLCM texture features represent how often a pixel with a specific grey level finds itself within a certain relationship to another pixel with another specific grey level [31, 36]. Until now, there have been few studies regarding GLCM texture parameter changes after neoadjuvant treatment and most of these studies have focused on the GLCM texture and tumor biology relationship. In previously published studies, the GLCM entropy of malignant pulmonary nodules was demonstrated to be higher compared to those of benign pulmonary nodules (3.800 vs. 3.560, $p = 0.001$) [31], and the GLCM entropy was significantly higher in high-grade gliomas than in low-grade gliomas (6.861 vs. 6.261, $p = 0.006$), based on the apparent diffusion coefficient (ADC) map [32]. We suggest that lower subtracted GLCM entropy related to lower preoperative tumor GLCM entropy is the important parameter for predicting longer OS. GLCM entropy is not simply a representation of heterogeneity, but a randomness of the matrix. For this reason, a smooth pattern will have low GLCM entropy and a checkerboard pattern which is not a textually uniform pattern will also have low GLCM entropy, even though these GLCM imaging features are not easily visible on the conventional grey-scale CT images [37, 38]. Further studies are required to evaluate the relationship between GLCM entropy change and histologic change and to confirm the role of GLCM entropy in the survival of PDAC patients.

Several limitations of our study need to be mentioned. First, as a retrospective study design, there may be a potential selection bias. Second, the radiologist performed manual segmentation. As an infiltrative feature of the PDAC margin,

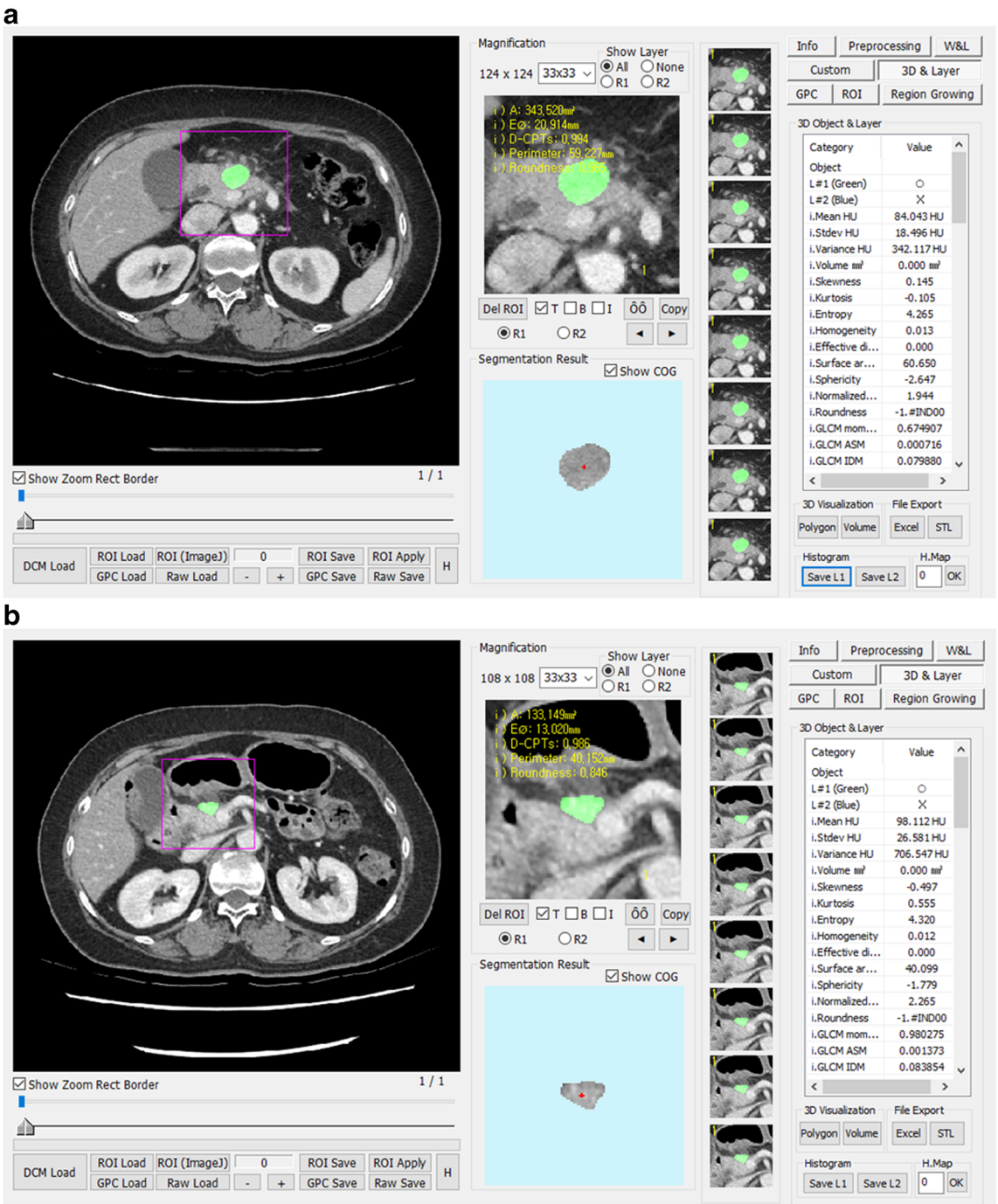

Fig. 4 **a**, **b** Comparison with CT texture analysis between baseline (**a**) and preoperative CT (**b**) in a 52-year-old man with a 2.5-cm pancreatic ductal adenocarcinoma. Segmentation and the texture features were extracted from baseline and preoperative CT images. The subtracted value of entropy of the pancreas head cancer was 0.0554 and the subtracted value of GLCM entropy was –0.3983. Overall survival was 35.3 months, which was longer than median survival (23.9 ±2.1 months)

especially after neoadjuvant treatment, automatic segmentation was technically challenging. And the manual segmentation technique is widely used in current texture analysis studies. Moreover, in order to minimize the influence of manual segmentation, consensus drawing and repetitive drawing of the ROI was performed. Third, postoperative adjuvant therapy could affect a patient's prognosis. Several trials showed an OS benefit in the adjuvant chemotherapy group, even though the effect of the additional radiation therapy remained controversial [39, 40]. However, in our study, most of the patients, except 6 patients including two patients who were followed up at outside hospital, received the adjuvant therapy and 29

patients received postoperative chemotherapy. So, the impact of the postoperative adjuvant therapy on our results would be minimal. Finally, as MDCT was performed using a number of different scanners in our study, inter-scanner difference might affect the texture analysis result. However, we excluded patients with different reconstruction techniques between the baseline and preoperative CT and all patients underwent similar CT protocols. Nevertheless, there are still some challenges to the clinical application as these results are from a retrospective analysis with different CT scanners. It might affect the texture analysis result. Therefore, further studies for inter-scanner variation of texture analysis need to be performed.

In conclusion, after neoadjuvant therapy, considering the borderline as resectable tumor has better accuracy for R0 resectability and particularly the neoadjuvant CCRT group provides better accuracy than the neoadjuvant chemotherapy group. In addition, CT texture analysis can be useful to predict a patient's prognosis after neoadjuvant therapy in PDAC.

Acknowledgement We also thank Bonnie Hami, M.A. (USA) for her editorial assistance in the preparation of this manuscript.

Funding The authors state that this work has not received any funding.

Compliance with ethical standards

Guarantor The scientific guarantor of this publication is Joon Koo Han, M.D.

Conflict of interest The authors of this manuscript declare no relationships with any companies, whose products or services may be related to the subject matter of the article.

Statistics and biometry Seo-Youn Choi MD has significant statistical expertise and no complex statistical methods were necessary for this paper.

Informed consent Written informed consent was waived by the institutional review board.

Ethical approval Institutional review board approval was obtained.

Study subjects or cohorts overlap Among 45 patients who were enrolled in our study, 13 patients have been previously reported in our previous paper (AJR Am J Roentgenol 2018, 210(5):1059–1065). However, the study purposes of these two studies were different. The previously published paper was a comparison of the diagnostic performance of CT in assessing tumor resectability pancreatic cancers after receiving neoadjuvant chemoradiation in comparison with those undergoing up-front surgery. The purpose of this study was to assess the utility of CT findings and texture analysis for predicting the resectability and prognosis in patients after neoadjuvant therapy for pancreatic cancer.

Methodology
- Retrospective
- Diagnostic or prognostic study
- Performed at one institution

References

1. Society AC (2017) Cancer facts & figures 2017. American Cancer Society, Atlanta
2. Sohn TA, Yeo CJ, Cameron JL et al (2000) Resected adenocarcinoma of the pancreas-616 patients: results, outcomes, and prognostic indicators. J Gastrointest Surg 4:567–579
3. Winter JM, Cameron JL, Campbell KA et al (2006) 1423 pancreaticoduodenectomies for pancreatic cancer: A single-institution experience. J Gastrointest Surg 10:1199–1210 discussion 1210–1191
4. Bilimoria KY, Talamonti MS, Sener SF et al (2008) Effect of hospital volume on margin status after pancreaticoduodenectomy for cancer. J Am Coll Surg 207:510–519
5. Neoptolemos JP, Stocken DD, Dunn JA et al (2001) Influence of resection margins on survival for patients with pancreatic cancer treated by adjuvant chemoradiation and/or chemotherapy in the ESPAC-1 randomized controlled trial. Ann Surg 234:758–768
6. Gillen S, Schuster T, Meyer Zum Buschenfelde C, Friess H, Kleeff J (2010) Preoperative/neoadjuvant therapy in pancreatic cancer: a systematic review and meta-analysis of response and resection percentages. PLoS Med 7:e1000267
7. McClaine RJ, Lowy AM, Sussman JJ, Schmulewitz N, Grisell DL, Ahmad SA (2010) Neoadjuvant therapy may lead to successful surgical resection and improved survival in patients with borderline resectable pancreatic cancer. HPB (Oxford) 12:73–79
8. Addeo P, Rosso E, Fuchshuber P et al (2015) Resection of Borderline Resectable and Locally Advanced Pancreatic Adenocarcinomas after Neoadjuvant Chemotherapy. Oncology 89:37–46
9. Soriano A, Castells A, Ayuso C et al (2004) Preoperative staging and tumor resectability assessment of pancreatic cancer: prospective study comparing endoscopic ultrasonography, helical computed tomography, magnetic resonance imaging, and angiography. Am J Gastroenterol 99:492–501
10. Somers I, Bipat S (2017) Contrast-enhanced CT in determining resectability in patients with pancreatic carcinoma: a meta-analysis of the positive predictive values of CT. Eur Radiol 27:3408–3435
11. Morgan DE, Waggoner CN, Canon CL et al (2010) Resectability of pancreatic adenocarcinoma in patients with locally advanced disease downstaged by preoperative therapy: a challenge for MDCT. AJR Am J Roentgenol 194:615–622
12. Cassinotto C, Cortade J, Belleannee G et al (2013) An evaluation of the accuracy of CT when determining resectability of pancreatic head adenocarcinoma after neoadjuvant treatment. Eur J Radiol 82:589–593
13. Kim YE, Park MS, Hong HS et al (2009) Effects of neoadjuvant combined chemotherapy and radiation therapy on the CT evaluation of resectability and staging in patients with pancreatic head cancer. Radiology 250:758–765
14. Cassinotto C, Mouries A, Lafourcade JP et al (2014) Locally advanced pancreatic adenocarcinoma: reassessment of response with CT after neoadjuvant chemotherapy and radiation therapy. Radiology 273:108–116
15. Ahn SJ, Kim JH, Park SJ, Han JK (2016) Prediction of the therapeutic response after FOLFOX and FOLFIRI treatment for patients with liver metastasis from colorectal cancer using computerized CT texture analysis. Eur J Radiol 85:1867–1874
16. Yip C, Landau D, Kozarski R et al (2014) Primary esophageal cancer: heterogeneity as potential prognostic biomarker in patients treated with definitive chemotherapy and radiation therapy. Radiology 270:141–148
17. Cassinotto C, Chong J, Zogopoulos G et al (2017) Resectable pancreatic adenocarcinoma: Role of CT quantitative imaging biomarkers for predicting pathology and patient outcomes. Eur J Radiol 90:152–158

18. Chee CG, Kim YH, Lee KH et al (2017) CT texture analysis in patients with locally advanced rectal cancer treated with neoadjuvant chemoradiotherapy: A potential imaging biomarker for treatment response and prognosis. PLoS One 12:e0182883
19. Goh V, Ganeshan B, Nathan P, Juttla JK, Vinayan A, Miles KA (2011) Assessment of response to tyrosine kinase inhibitors in metastatic renal cell cancer: CT texture as a predictive biomarker. Radiology 261:165–171
20. Callery MP, Chang KJ, Fishman EK, Talamonti MS, William Traverso L, Linehan DC (2009) Pretreatment assessment of resectable and borderline resectable pancreatic cancer: expert consensus statement. Ann Surg Oncol 16:1727–1733
21. Loyer EM, David CL, Dubrow RA, Evans DB, Charnsangavej C (1996) Vascular involvement in pancreatic adenocarcinoma: reassessment by thin-section CT. Abdom Imaging 21:202–206
22. Tempero MA, Arnoletti JP, Behrman SW et al (2012) Pancreatic Adenocarcinoma, version 2.2012: featured updates to the NCCN Guidelines. J Natl Compr Cancer Netw 10:703–713
23. Sobin L, Gospodarowicz MK, Wittekind C (2010) International Union against Cancer TNM classification of malignant tumors, 7th ed. 2009 edn. Wiley-Blackwell, Chichester
24. Eilaghi A, Baig S, Zhang Y et al (2017) CT texture features are associated with overall survival in pancreatic ductal adenocarcinoma - a quantitative analysis. BMC Med Imaging 17:38
25. Chae HD, Park CM, Park SJ, Lee SM, Kim KG, Goo JM (2014) Computerized texture analysis of persistent part-solid ground-glass nodules: differentiation of preinvasive lesions from invasive pulmonary adenocarcinomas. Radiology 273:285–293
26. Katz MH, Fleming JB, Bhosale P et al (2012) Response of borderline resectable pancreatic cancer to neoadjuvant therapy is not reflected by radiographic indicators. Cancer 118:5749–5756
27. White RR, Paulson EK, Freed KS et al (2001) Staging of pancreatic cancer before and after neoadjuvant chemoradiation. J Gastrointest Surg 5:626–633
28. Ng F, Ganeshan B, Kozarski R, Miles KA, Goh V (2013) Assessment of primary colorectal cancer heterogeneity by using whole-tumor texture analysis: contrast-enhanced CT texture as a biomarker of 5-year survival. Radiology 266:177–184
29. Ng F, Kozarski R, Ganeshan B, Goh V (2013) Assessment of tumor heterogeneity by CT texture analysis: can the largest cross-sectional area be used as an alternative to whole tumor analysis? Eur J Radiol 82:342–348
30. Chee CG, Kim YH (2017) CT texture analysis in patients with locally advanced rectal cancer treated with neoadjuvant chemoradiotherapy: A potential imaging biomarker for treatment response and prognosis. 12:e0182883
31. Zhao Q, Shi CZ, Luo LP (2014) Role of the texture features of images in the diagnosis of solitary pulmonary nodules in different sizes. Chin J Cancer Res 26:451–458
32. Ryu YJ, Choi SH, Park SJ, Yun TJ, Kim JH, Sohn CH (2014) Glioma: application of whole-tumor texture analysis of diffusion-weighted imaging for the evaluation of tumor heterogeneity. PLoS One 9:e108335
33. Yip C, Davnall F, Kozarski R et al (2015) Assessment of changes in tumor heterogeneity following neoadjuvant chemotherapy in primary esophageal cancer. Dis Esophagus 28:172–179
34. Chatterjee D, Katz MH, Rashid A et al (2012) Histologic grading of the extent of residual carcinoma following neoadjuvant chemoradiation in pancreatic ductal adenocarcinoma: a predictor for patient outcome. Cancer 118:3182–3190
35. Hartman DJ, Krasinskas AM (2012) Assessing treatment effect in pancreatic cancer. Arch Pathol Lab Med 136:100–109
36. Zhan Y, Shen D (2006) Deformable segmentation of 3-D ultrasound prostate images using statistical texture matching method. IEEE Trans Med Imaging 25:256–272
37. Albregtsen F (2008) Statistical texture measures computed from gray level coocurrence matrices. Image Processing Laboratory, Department of Informatics, University of Oslo Web site; Available via http://www.uio.no/studier/emner/matnat/ifi/INF4300/h08/undervisningsmateriale/glcm.pdf
38. Partio M, Cramariuc B, Gabbouj M, Visa A (2002) Rock texture retrieval using gray level co-occurrence matrix Proc of 5th Nordic Signal Processing Symposium
39. Oettle H, Neuhaus P, Hochhaus A et al (2013) Adjuvant chemotherapy with gemcitabine and long-term outcomes among patients with resected pancreatic cancer: the CONKO-001 randomized trial. JAMA 310:1473–1481
40. Neoptolemos JP, Stocken DD, Friess H et al (2004) A randomized trial of chemoradiotherapy and chemotherapy after resection of pancreatic cancer. N Engl J Med 350:1200–1210